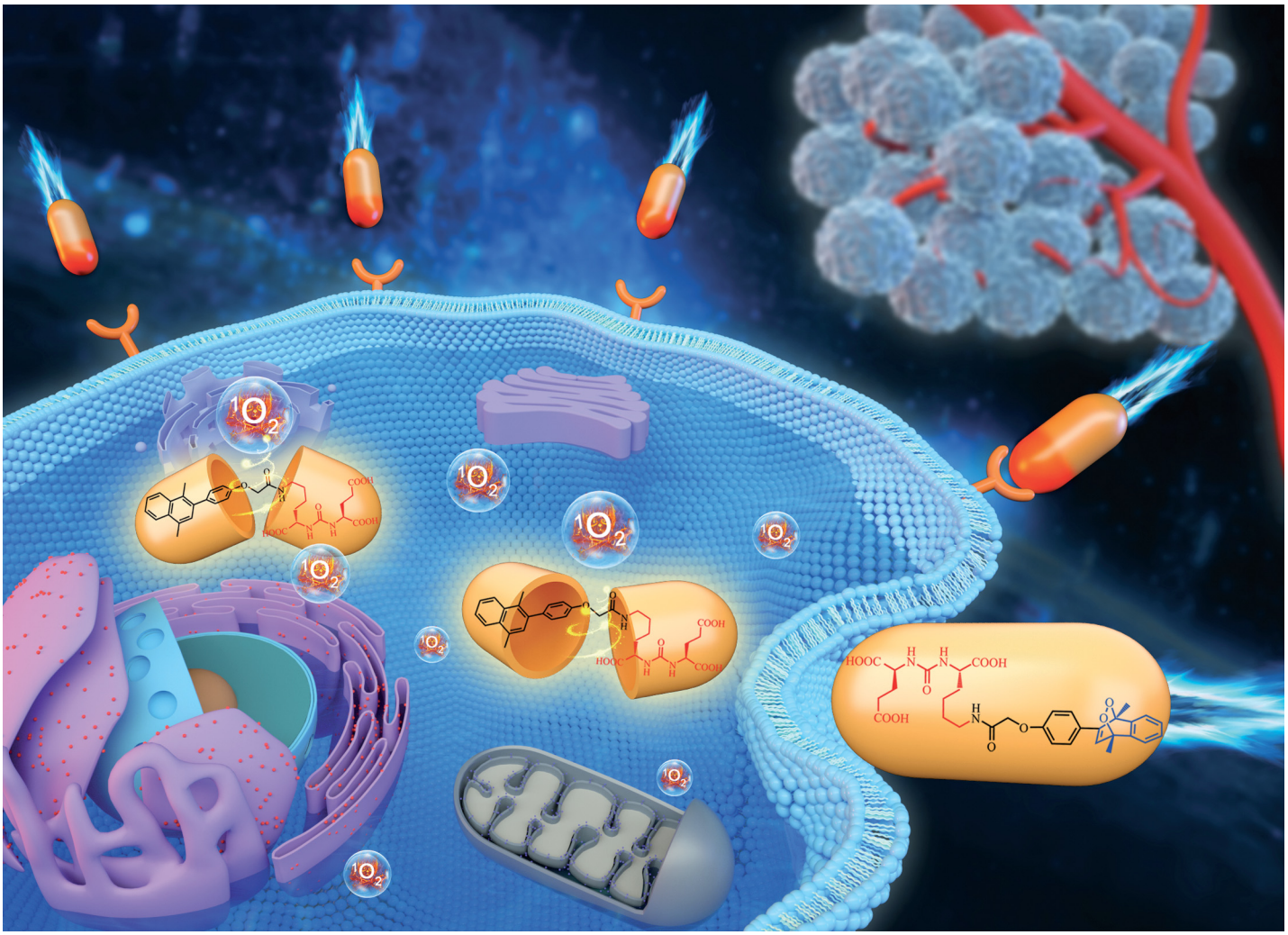

Showcasing research from Professor Akkaya's laboratory, State Key Laboratory of Fine Chemicals and Department of Pharmaceutical Science, Dalian University of Technology, Dalian, People's Republic of China.

Prostate-specific membrane antigen (PSMA) targeted singlet oxygen delivery *via* endoperoxide tethered ligands

A ligand with high affinity for PSMA makes endoperoxides effective cytotoxic agents selective for prostate cancer cells, providing further evidence that the targeted release of singlet oxygen is likely to deliver significant therapeutic benefits.

As featured in:

See Yue Pan, Engin U. Akkaya *et al.*, *Chem. Commun.*, 2022, **58**, 1902.

ROYAL SOCIETY OF CHEMISTRY

rsc.li/chemcomm

Registered charity number: 207890

ChemComm

COMMUNICATION

View Article Online
View Journal | View Issue

Cite this: *Chem. Commun.*, 2022, **58**, 1902

Received 15th October 2021,
Accepted 22nd December 2021

DOI: 10.1039/d1cc05810j

rsc.li/chemcomm

Prostate-specific membrane antigen (PSMA) targeted singlet oxygen delivery *via* endoperoxide tethered ligands†

Lei Wang, Lei Tang, Yingjie Liu, Hao Wu, Ziang Liu, Jin Li, Yue Pan* and Engin U. Akkaya *

Singlet oxygen is the primary agent responsible for the therapeutic effects of photodynamic therapy (PDT). In this work, we demonstrate that singlet oxygen release due to thermal endoperoxide cycloreversion can be targeted towards specific features of selected cancer cells, and this targeted singlet oxygen delivery can serve as an effective therapeutic tool. Thus, cytotoxic singlet oxygen can be delivered regioselectively into prostate specific membrane antigen (PSMA) overexpressing lymph node carcinoma (LNCaP) cells. However, unlike typical photodynamic processes, there is no need for light or oxygen. The potential of the approach is exciting, considering the limitations on the availability of light and oxygen in deep-seated tumors.

Singlet oxygen is a reactive oxygen species (ROS) which can be generated photochemically, chemically or enzymatically, both *in vitro* and *in vivo*.[1] In aqueous solutions, the half-life of singlet oxygen is about 3.5 microseconds. It is believed to have a very short diffusion distance *in vivo*, as short as 10–20 nm, according to certain estimates.[2] This short lifetime is mostly due to physical quenching with biomolecules,[3] rather than water inside the cells. Thus, if the generation (or release) of singlet oxygen can be spatially controlled, a very precise therapeutic tool can be obtained.

In recent years, controlled release of singlet oxygen has attracted attention.[4] Previously, we proposed[4b,5] that chemically and biochemically triggered singlet oxygen release from endoperoxides may have important therapeutic implications (Targeted Singlet Oxygen Delivery, or TSOD) by essentially providing the benefits of PDT, without its limitations.

Prostate cancer (PCa) is the second-leading cause of cancer mortality in men.[6] Prostate specific membrane antigen (PSMA) is a transmembrane protein and a metalloenzyme,[7] which is highly expressed in the prostate, but is expressed up to 12-fold more in a cancerous prostate. PSMA levels correlate with the proliferation, migration, invasion, adhesion and survival characteristics of cancer cells.[8] Thus, not surprisingly, this protein is targeted in a number of therapeutic schemes.[9]

A large variety of ligands were tested for their affinity to PSMA.[10] Typically, once the ligand binds to the target, the PSMA–ligand complex undergoes endocytosis and unloads the ligand, then it is recycled back to the membrane.[11] Most of these ligands contain a particular unit abbreviated as *KuE* (lysine–urea–glutamate) which targets the active site of the protein. Among them, PSMA-617 was found to be highly promising, and making use of its chelator DOTA unit, the $^{177}Lu^{3+}$ complex of PSMA-617 has undergone clinical tests against certain types of prostate cancers (Fig. 1).[12]

Here, in this work, we targeted a PCa associated protein, prostate specific membrane antigen (PSMA), with

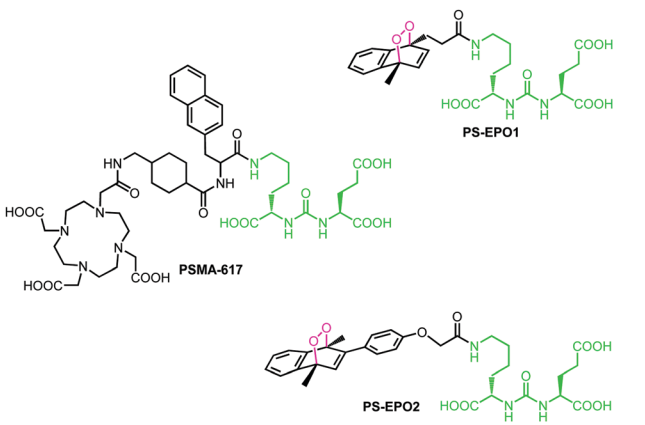

Fig. 1 Structures of the ligand **PSMA-617** and the endoperoxide compounds **PS-EPO1** and **PS-EPO2** described in this work. All three compounds have naphthalene or naphthalene-derived endoperoxide units and the Lys–urea–Glu (*KuE*) structural motif (highlighted in green).

State Key Laboratory of Fine Chemicals, Department of Pharmaceutical Science, Dalian University of Technology, 2 Linggong Road, Dalian, Liaoning, 116024, China. E-mail: panyue0811@dlut.edu.cn, eua@dlut.edu.cn

† Electronic supplementary information (ESI) available: Experimental procedures, characterization data of compounds, copies of NMR spectra for the synthesized compounds and biological data. See DOI: 10.1039/d1cc05810j

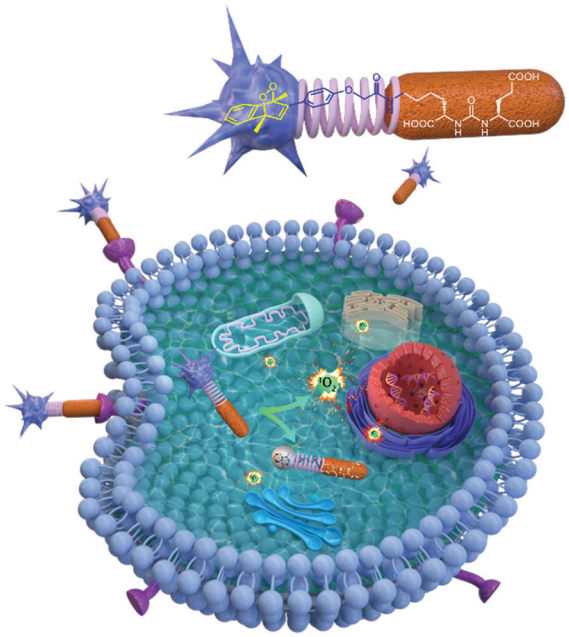

Fig. 2 Metastable endoperoxide is targeted to PSMA overexpressing cancer cells, where it is internalized by endocytosis. Thermally (@37 °C) released singlet oxygen then attacks cellular targets, including organellar membranes. The endoperoxide depicted here is **PS-EPO2**.

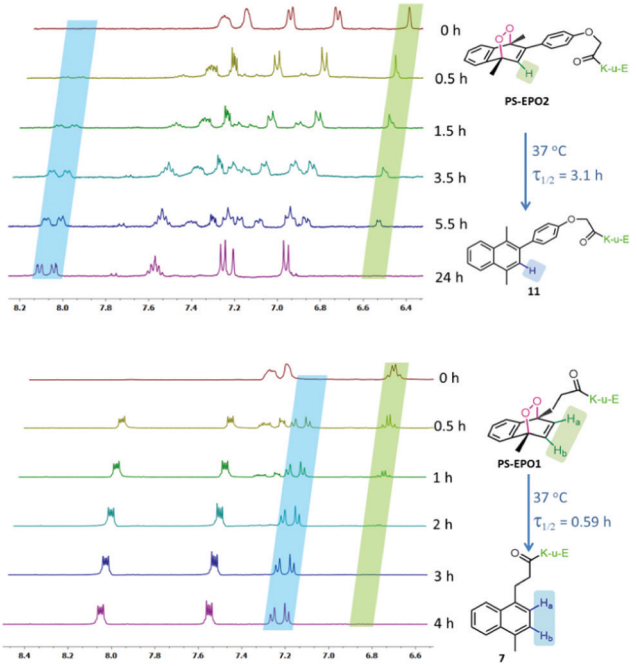

Fig. 3 Temporal evolution of partial ^{1}H NMR spectra of **PS-EPO2** (top) and **PS-EPO1** (bottom) in D_2O at 37 °C.

ligand–endoperoxide conjugates. The PSMA ligand (*KuE*) carries a naphthalene derived unit; thus, we surmised that the naphthalene endoperoxide structure to be substituted will only cause minimal structural changes, and thus not impact the affinity of the ligand for PSMA. The endocytosed ligand–endoperoxide conjugate would thermally release singlet oxygen into the cytosol of targeted cancer cells (Fig. 2).

With these considerations, naphthalene precursors of **PS-EPO1** and **PS-EPO2** (compounds 7 and **11**, shown in Fig. 3) were synthesized from commercially available materials in good yields (see the ESI†). With these two precursors in hand, we synthesized the corresponding endoperoxides **PS-EPO1** and **PS-EPO2** by irradiation of compounds 7 and **11**, respectively, in the presence of methylene blue using a 630 nm LED array in D_2O. After completion of the reactions, photosensitizer methylene blue was then removed using a cation exchange resin.

Our choice of the two structurally different naphthalene endoperoxides **PS-EPO1** and **PS-EPO2** was guided by an understanding of the effects of substitution on the rates of cycloreversion reactions.[13] It was reported[13b] that phenyl substitution at the 2 position of the endoperoxide slows down the rate up to 10-fold compared to the parent compound (1,4-dimethyl-1,4-endoperoxide). The rate of singlet oxygen release may be a more important parameter than the total amount of singlet oxygen released, because of the dynamic nature of the cells, with many interlinked non-equilibrium processes.[14]

We studied the rate of cycloreversion of both compounds **PS-EPO1** and **PS-EPO2** using ^{1}H NMR, and the results are shown in Fig. 3. The NMR spectra in the aromatic region have relatively isolated peaks, which allow us to follow the reaction. The NMR spectra show the cycloreversion of **PS-EPO1**. The peaks between 6.8 and 6.9 ppm are from the two protons in the endoperoxide ring (H_a and H_b) and the newly generated peaks between 7.2 and 7.3 ppm belong to its naphthalene precursor (7). This result clearly indicated that endoperoxide **PS-EPO1** was converted to its naphthalene precursor 7 within 4 hours. A similar result was obtained when **PS-EPO2** was tested by the same procedure. When incubated at 37 °C in D_2O, the half-life of **PS-EPO1** is 0.59 h, whereas **PS-EPO2** has a half-life of 3.1 h. As expected, the endoperoxide with a phenyl substitution at the 2-position (**PS-EPO2**) has a longer half-life compared to **PS-EPO1**. NMR data also showed that cycloreversion to naphthalene precursors proceeds without any undesirable by-products, with molecular oxygen as the only other product.

In order to confirm that the release of oxygen is in the excited state (singlet oxygen) and at different rates with these two endoperoxides, we monitored the reaction using the singlet oxygen probe SOSG (Singlet Oxygen Sensor Green), following the spectral changes (Fig. 4). The cycloreversion rate differences are reflected in the rate of increase of fluorescence changes of SOSG in buffered solutions. While **PS-EPO1** releases singlet oxygen much faster compared to **PS-EPO2**, the total amount of singlet oxygen trapped with the probe is comparable.

The binding affinities of the endoperoxides were determined by an ELISA (Fig. 5 and ESI†). As expected, both compounds showed strong PSMA affinity with equilibrium dissociation constants near 20 nM.

Before we tested the activity of the two PSMA-targeting endoperoxides, we wanted to demonstrate enhanced expression of PSMA in LNCaP cells compared to two other prostate cells with known lower expression of PSMA (PC3, DU145).

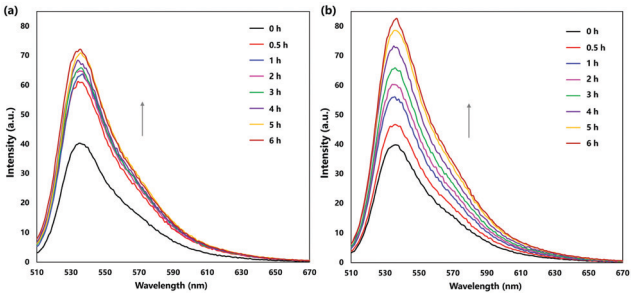

Fig. 4 Thermal singlet oxygen release by (a) **PS-EPO1** and (b) **PS-EPO2** as monitored using the SOSG probe. Emission spectra were acquired by excitation at 488 nm.

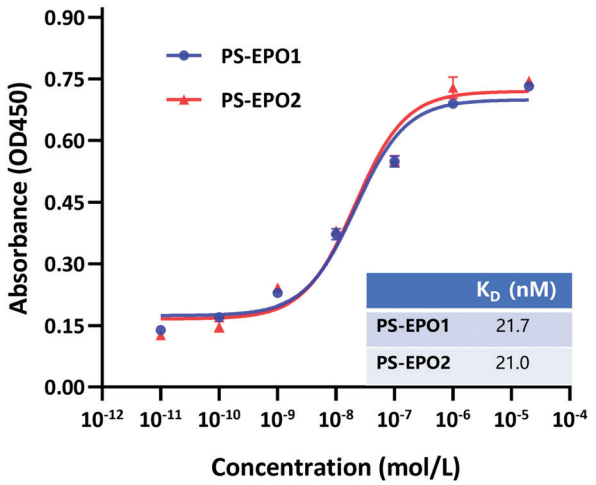

Fig. 5 PSMA-based ELISA to determine the binding affinity of **PS-EPO1** and **PS-EPO2** for the PSMA protein. The K_D data were calculated using GraphPad Prism.

This was confirmed by western blot analysis for the PSMA which showed larger PSMA expression in the cell extracts and membrane enriched extracts of LNCaP cells, as expected, compared to the other two prostate cancer cell lines (PC3 and DU145) (Fig. 6). β-Actin is the internal reference protein. In addition, we carried out immunostaining imaging, showing the expression levels of PMSA (ESI,† Fig. S17).

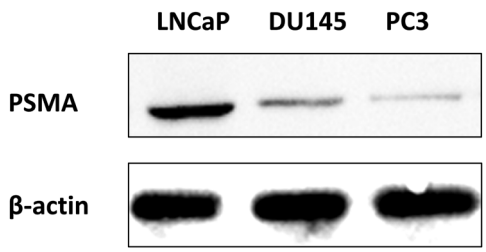

Fig. 6 Western blot analysis for detection of PSMA expression in LNCaP, DU145, and PC3 cell membranes, in comparison to internal reference β-actin.

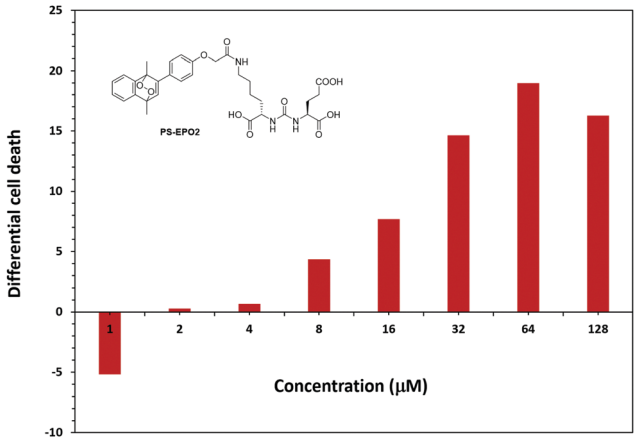

Fig. 7 Percentage cell death difference (LNCaP-PC3) due to **PS-EPO2** as determined by MTT assays with LNCaP and PC3. The cell death is larger in LNCaP cells except for the 1 μM data point.

MTT assays of cell viability also produce results confirming the validity of our approach. First, the endoperoxide precursor compounds **7** and **11** show negligible cytotoxicity towards all three cell lines tested. However, endoperoxide **PS-EPO1** and especially **PS-EPO2** discriminate between PSMA overexpressing LNCaP cell lines and the others (Fig. 7 and ESI†). As expected, the cytotoxicity is more pronounced towards LNCaP, and the difference in cell death is 20% more than PC3 cells. Among the endoperoxides **PS-EPO1** and **PS-EPO2**, the latter compound seems to be more effective, possibly due to its longer half-life. The IC_{50} of **PS-EPO2** was determined to be 60 μM with LNCaP cells, whereas for PC3 cells it is larger than 200 μM.

In order to eliminate any inhibitory effects as part of the PSMA mediated toxicity, we compared the activities of the precursor naphthalene compound **11** and **PS-EPO2** (Fig. 8). For all cell types, cytotoxicity is mostly due to singlet oxygen, but the singlet oxygen toxicity is the most effective for PSMA overexpressing LNCaP cells.

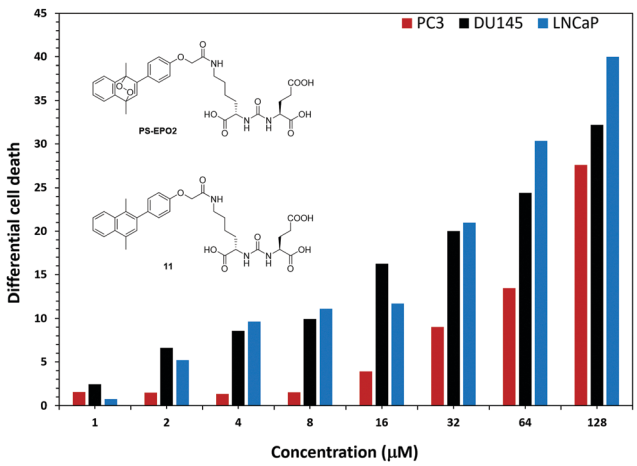

Fig. 8 The difference in cell death as determined by MTT assays between the endoperoxide compound **PS-EPO2** and the precursor naphthalene **11** at the indicated concentrations.

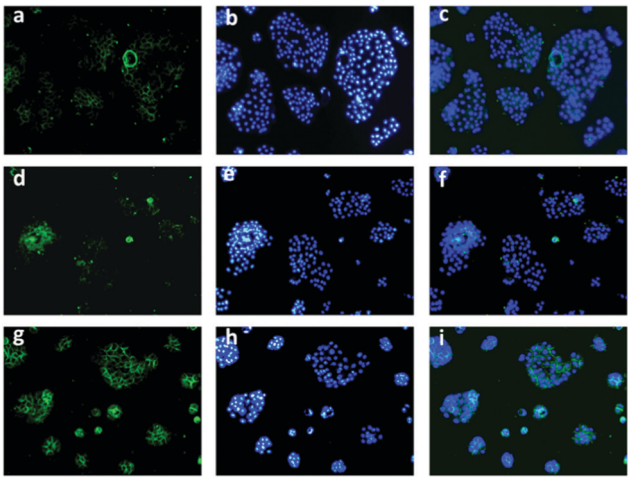

Fig. 9 Microscopy images of cell cultures treated with **PS-EPO2**. First row (a–c): PC3 cells, second row (d–f): DU145 cells, and third row (g–i): LNCaP cells. First column (a, d and g): ROS imaging with DCFH-DA, second column (b, e and h): nuclear staining with DAPI, and third column (c, f and i): merged images.

To track the generation of singlet oxygen in living cells, an imaging experiment was conducted with a commonly used ROS indicator, 2′,7′-dichlorodihydrofluorescein diacetate (DCFH-DA), by CLSM. When PC3 cells which express lower PSMA were treated with DCFH-DA and **PS-EPO2** accordingly, weak fluorescence emission was detected, indicating the existence of endogenous singlet oxygen (Fig. 9). Inspired by this result, DU145 and LNCaP cells were tested according to the same procedure. As expected, LNCaP cells with enhanced expression of PSMA showed significant green fluorescence compared to the other two cell lines. It was indicated that a larger amount of singlet oxygen is trapped by the probe when the LNCaP cells are incubated with **PS-EPO2** compared to the other cell types. This is in accordance with our expectations of enhanced PSMA-mediated endocytosis for the singlet oxygen releasing compound.

Also, in the absence of endoperoxides, all three cell types showed no or hardly discernable emission following ROS probe incubation (ESI,† Fig. S24), further confirming that the sources of the ROS (singlet oxygen) are the endoperoxide compounds.

In conclusion, we developed a PSMA-targeted singlet oxygen delivery system. The endoperoxide modified ligand shows good inhibition towards PSMA overexpressing LNCaP cells. Comprehensive design of endoperoxide structures allows us to control the release ratio of singlet oxygen and it is clear that the rate of singlet oxygen delivery and the exact location of the singlet oxygen release can be important parameters in optimizing the effectiveness of the proposed method. We demonstrated that Targeted Singlet Oxygen Delivery (TSOD) can be an effective tool for cancer therapy, and our work in establishing this approach is in progress.

The authors acknowledge financial support from the Liao-Ning Revitalization Talents Program (E. U. A.: XLYC1902001, L. W.: XLYC1907021) and the National Natural Science Foundation of China (L. W.: 22007008, Y. P.: 81803024).

Conflicts of interest

There are no conflicts to declare.

Notes and references

1 Y. You, *Org. Biomol. Chem.*, 2018, **16**, 4044–4060.
2 (*a*) P. Di Mascio, G. R. Martinez, S. Miyamoto, G. E. Ronsein, M. H. G. Medeiros and J. Cadet, *Chem. Rev.*, 2019, **119**, 2043–2086; (*b*) P. Ogilby, *Photochem. Photobiol. Sci.*, 2010, **9**, 1543–1560; (*c*) M. Bregnhøj, M. Westberg, F. Jensen and P. R. Ogilby, *Phys. Chem. Chem. Phys.*, 2016, **18**, 22946–22961.
3 A. Baker and J. R. Kanofsky, *Photochem. Photobiol.*, 1992, **55**, 523–528.
4 (*a*) W. Fudickar and T. Linker, *ChemPhotoChem*, 2018, **2**, 548–558; (*b*) E. Ucar, D. Xi, O. Seven, C. Kaya, X. J. Peng, W. Sun and E. U. Akkaya, *Chem. Commun.*, 2019, **55**, 13808–13811; (*c*) M. Qu, N. Wu, W. Q. Jiang, L. Wang, M. S. Akkaya and E. U. Akkaya, *RSC Adv.*, 2021, **11**, 19083–19087.
5 (*a*) S. Kolemen, T. Ozdemir, D. Lee, G. M. Kim, T. Karatas, J. Yoon and E. U. Akkaya, *Angew. Chem., Int. Ed.*, 2016, **55**, 3606–3610; (*b*) I. S. Turan, D. Yildiz, A. Turksoy, G. Gunaydin and E. U. Akkaya, *Angew. Chem., Int. Ed.*, 2016, **55**, 2875–2878; (*c*) S. Ayan, G. Gunaydin, N. Yesilgul-Mehmetcik, M. E. Gedik, O. Seven and E. U. Akkaya, *Chem. Commun.*, 2020, **55**, 14793–14796.
6 F. Bray, J. Ferlay, I. Soerjomataram, R. L. Siegel, L. A. Torre and A. Jemal, *CA-Cancer J. Clin.*, 2018, **68**, 394–424.
7 R. G. Lapidus, C. W. Tiffany, J. T. Isaacs and B. S. Slusher, *Prostate*, 2000, **45**, 350–354.
8 (*a*) Y. Zhang, Z. Guo, T. Du, J. Chen, W. Wang, K. Xu, T. Lin and H. Huang, *Prostate*, 2013, **73**, 835–841; (*b*) J. S. Ross, C. E. Sheehan, H. A. G. Fisher, R. P. Kaufman Jr., P. Kaur, K. Gray, I. Webb, G. S. Gray, R. Mosher and B. V. S. Kallakury, *Clin. Cancer Res.*, 2003, **9**, 6357–6362.
9 (*a*) A. P. Kiess, S. R. Banerjee, R. C. Mease, S. P. Rowe, A. Rao, C. A. Foss, Y. Chen, X. Yang, S. Y. Cho, S. Nimmagadda and M. G. Pomper, *Q. J. Nucl. Med. Mol. Imaging*, 2019, **59**, 241–268; (*b*) A. Cimadamore, M. Cheng, M. Santoni, A. Lopez-Beltran, N. Battelli, F. Massari, A. B. Galosi, M. Scarpelli and R. Montironi, *Front. Oncol.*, 2018, **8**, 653.
10 M. Eiber, W. P. Fendler, S. P. Rowe, J. Calais, M. S. Hofman, T. Maurer, S. M. Schwarzenboeck, C. Kratowchil, K. Herrmann and F. L. Giesel, *J. Nucl. Med.*, 2017, **58**, 67S–76S.
11 (*a*) J. Roy, T. X. Nguyen, A. K. Kanduluru, C. Venkatesh, W. Lv, P. V. Reddy, P. S. Low and M. Cushman, *J. Med. Chem.*, 2015, **58**, 3094–3103; (*b*) H. Liu, A. K. Rajasekaran, P. Moy, Y. Xia, S. Kim, V. Navarro, R. Rahmati and N. H. Bander, *Cancer Res.*, 1998, **58**, 2674–2681.
12 M. J. Morris, J. S. De Bono, K. N. Chi, K. Fizazi, K. Herrmann, K. Rahbar, S. T. Tagawa, L. T. Nordquist, N. Vaishampayan, G. El-Haddad, C. H. Park, T. M. Beer, W. J. Pérez-Contreras, M. Desilvio, E. E. Kpamegan, G. Gericke, R. A. Messmann, B. J. Krause and A. O. Sartor, *J. Clin. Oncol.*, 2021, **39**, LBA4–LBA4.
13 (*a*) H. H. Wasserman, K. B. Wiberg, D. L. Larsen and J. Parr, *J. Org. Chem.*, 2005, **70**, 105–109; (*b*) M. Klapper and T. Linker, *Chem. – Eur. J.*, 2015, **21**, 8569–8577.
14 S. Ornes, *Proc. Natl. Acad. Sci. U. S. A.*, 2017, **114**, 423–424.